

# Spectroscopy Of Low Metallicity Giant H II Regions: A grid of low Metallicity Stellar atmospheres

S.L. Pistinner<sup>1</sup>, P. H. Hauschildt<sup>2</sup>, D. Eichler<sup>3</sup> & E. A. Baron<sup>4</sup>

<sup>1</sup>*Dept. of Applied Mathematics Israel Institute for Biological Research  
P.O.B 19 Nes-Ziona 74100 Israel*

<sup>2</sup>*Dept. of Physics & Astronomy, The University of Georgia, Athens, GA 30602-2451, USA  
yeti@hal.physast.uga.edu*

<sup>3</sup>*Department of Physics, Ben-Gurion University Beer-Sheba, 84105, Israel  
eichler@bgwms.bgu.ac.il*

<sup>4</sup>*Dept. of Physics & Astronomy, University of Oklahoma, Norman OK 73019-0225, USA  
baron@mail.nhn.ou.edu*

Accepted xx. Received xx

## ABSTRACT

We calculate a grid of spherically symmetric OB stellar atmospheres at low metallicities, including both non-local thermodynamic equilibrium (NLTE) and metal line blanketing effects. This is done to assess the uncertainties in helium abundance determination by nebular codes due to input stellar atmosphere models. The more sophisticated stellar atmosphere models we use can differ from LTE models by as much as 40 percent in the ratio of He to H-ionizing photons.

**Key words:** galaxies:abundances-galaxies:irregular-H II regions

## 1 INTRODUCTION

Giant extra-galactic H II regions (GEHR) are interesting objects for many reasons (cf. Shields 1990 for a review). However, low metallicity HII regions draw the most attention. This subgroup of low metallicity GEHR is believed to have had little chemical evolution over a Hubble time. Therefore, it is widely accepted that GEHR offer an opportunity to measure the primordial chemical composition of the universe.

The primordial composition of the universe is predicted by big-bang nucleosynthesis theory. If low metallicity GEHR provide a way to determine the primordial element abundance then they allow testing of some big-bang cosmology predictions, in particular the primordial helium abundance  $Y^P$ , which has implications for the baryonic fraction of matter in the universe and may limit the number of exotic light particle species. Although low metallicity GEHR show little chemical evolution, some chemical evolution did take place over a Hubble time, thereby requiring an extrapolation of the “measured” helium abundance  $Y^{obs}$  (as a function of the observed metallicity) to zero metallicity. This procedure yields the value of  $Y^P$ , the quantity of interest. The extrapolation techniques to zero metallicity are discussed by Pegal et. al. (1992). In this paper we concentrate on systematic errors in the determination of  $Y^{obs}$  from low metallicity GEHR introduced by systematic changes of the radiation field that ionizes the nebula.

The use of nebular spectroscopy to measure element

abundance is model dependent. The internal physics of GEHR is therefore of prime importance. The uncertainties include: a) the spectrum of the ionizing low metallicity stars, b) the filamentary structure of GEHR, c) supersonic turbulence inferred from radio observations, d) radiative transfer effects within the nebula (Terlevich, Skillman & Terlevich 1995 ;Sasselov & Goldwirth 1995).

The uncertainty of  $Y^{obs}$  determinations is required to be no more than several percent in order to derive accurate enough values of  $Y^P$  for, say, establishing the number of light neutrino species. Typically the value of  $Y^{obs}$  is derived from recombination lines of singly and doubly ionized helium (Skillman et al. 1994) which are compared to  $H_\alpha$  emission. This implies that an essential assumption is that the fraction of neutral helium in the nebula is negligible. If the fraction of neutral Helium is several percent, then the value of  $Y^{obs}$  cannot be determined to the required accuracy. Therefore, the helium ionization degree in H II regions has been the subject of numerous meticulous studies. Two problems are often mentioned in this context: i) the filamentary structure of the nebula and ii) the uncertainties in the underlying ionizing (stellar) radiation field. The latter uncertainties can translate into uncertainties in relative sizes of the He and H ionization zones.

This paper does not attempt to deal with problems associated with the filamentary structure of the nebula. However, the existence of this problem must be noted. It is observationally established that most of the line emission of

arXiv:astro-ph/9811021v1 2 Nov 1998

GEHR comes from a rather small filamentary volume. The volume filling factor of these filaments is about 1%. They move relative to each other with a velocity dispersion which is supersonic. Moreover, radio observations reveal that in about half of the H II regions in M51 (not a low metallicity region) the radio emission originates in a non-thermal component within the filaments. The origin and dynamics of the filaments are not fully understood. Clearly, if they contain any neutral or singly ionized He, then the He/H abundance determination is hindered by this source of inaccuracy. Thus, before any final statement can be made, one requires strong observational constraints of the properties of the matter in these filaments or a reliable theoretical model to understand the origin and the detailed physics of the filaments.

Due to the complexity of the nebular filamentary structure most authors have invoked homogeneous nebular models, in slab or spherical geometry. These spherical and shell homogeneous models constrain the ionization degree of helium to be 0.98 if the effective temperature of the ionizing stars is above 38,000K (Dinerstein & Shields 1986; Skillman 1989). However, these authors note that if the GEHR is actually an ensemble of much smaller H II regions which are ionized by stars of different effective temperatures (lower than 38,000K, Dinerstein 1989), filamentary neutral helium structures might form within the nebula. Even if this problem is ignored and one assumes that all ionizing stars have effective temperatures above 38,000K, there are uncertainties due to a lack of a state-of-the-art grid of model atmospheres in the required range of interest (Shields 1990). Recently, some effort has been put into this problem by (Garacía-Vargas 1996; Garacía-Vargas et al. 1997). They attempt to account for the filamentation by using shell models of the nebula, then, using the photo-ionization code CLOUDY (Ferland 1996), they fit the stellar and nebular spectra self-consistently. They conclude (Garacía-Vargas et al. 1997) that contamination from young evolved stellar population e.g. Wolf-Rayet stars, is of importance and must be taken into account.

The need for consistent spectral modeling of GEHR has been recognized by (Garacía-Vargas & Díaz 1994), who have used (Kurucz 1992) LTE line blanketed models with a range of abundances as input to CLOUDY. However, they express their concern that NLTE effects might become important in the relevant range of parameters. This lack of state-of-the-art NLTE line blanketed model stellar atmospheres is troubling, because most of the ionizing spectra of the nebula is in the UV range, which is strongly metal line blanketed. Typically for solar abundance stars, photons in this spectral region are strongly affected by the presence of many spectral lines. Yet, the input stellar model atmospheres used so far assumed either a pure hydrogen helium mixture in NLTE, or assumed LTE for the metal lines. This introduced a source of uncertainty that this paper addresses. In addition, (Kurucz 1994) has improved and modified the line data set of (Kurucz 1992), and these effects are taken into account as well.

There is already a substantial literature on non-LTE effects (some of the classical papers are: Auer & Mihalas 1972, Kudritzki 1973, 1976, 1979, 1988, Husfeld et al. 1984). Our purpose here is to evaluate their contribution to the uncertainties in He abundance determination. In recent years stellar atmosphere and radiative transfer codes have become very sophisticated in a way which allows much

more of the important physics to be taken into account. We use such a code to construct a grid of low-metallicity hot stellar atmosphere models including NLTE and metal line blanketing. This allows us to assess and reduce one of the uncertainties in the determination of  $Y^{obs}$ . We provide the spectra of these models in machine readable format at <http://dilbert.physast.uga.edu/~yeti>.

The structure of this paper is as follows: in § 2 we discuss briefly the stellar atmosphere code PHOENIX, and describe in detail the input physics of stellar spectrum models. We then provide in § 3 some examples of the variation of the spectrum in the UV range. We present the ionization parameters of helium and hydrogen, depending on various assumptions, and assess the variation of these quantities as functions of the stellar atmosphere model input parameters. We summarize our conclusions in § 4.

## 2 METHODS AND MODELS

In order to investigate the importance of NLTE effects on the formation of OB star spectra and ionizing photon fluxes, full and very detailed NLTE model calculations are required in order to model the effects of NLTE on the very important EUV and UV metal lines. This means that the multi-level NLTE rate equations must be solved self-consistently and simultaneously with the radiative transfer and energy equations, including the effects of line blanketing and the extension of the atmosphere. For the purpose of this analysis we use our multi-purpose stellar atmosphere code PHOENIX. PHOENIX [version 9.1 (Hauschildt et al. 1996; Hauschildt et al. 1997; Hauschildt, Baron, & Allard 1997; Baron & Hauschildt 1998)] uses a special relativistic spherical radiative transfer and an equation of state (EOS) including more than 300 atoms and ions (39 elements with up to 26 ionization stages). The temperature correction is based on a modified (for NLTE and scattering) Unsöld-Lucy method that converges quickly and is numerically stable. See (Hauschildt & Baron 1996) for details on the numerical methods used in PHOENIX.

Both the NLTE and LTE (background) lines are treated with a direct opacity sampling method. However, we do *not* use pre-computed opacity sampling tables. We dynamically select the relevant LTE background lines from master line lists at the beginning of each iteration and sum up the contribution of every line to compute the total line opacity at *arbitrary* wavelength points. The latter is crucial in NLTE calculations in which the wavelength grid is both irregular and variable (from iteration to iteration due to changes in the physical conditions). This approach also allows detailed and depth dependent line profiles to be used during the iterations. To make this method computationally efficient, we employ modern numerical techniques, e.g., vectorized and parallel block algorithms with high data locality (Hauschildt, Baron, & Allard 1997), and we use high-end workstations or parallel supercomputers for the model calculations. In the calculations we present in this paper, we have set the statistical (treated as micro-turbulence) velocity  $\xi$  to  $2 \text{ km s}^{-1}$ . We include LTE background lines (i.e., lines of species that are not treated explicitly in NLTE) if they are stronger than a threshold  $\Gamma \equiv \chi_l/\kappa_c = 10^{-4}$ , where  $\chi_l$  is the extinction coefficient of the line at the line center

and  $\kappa_c$  is the local b-f absorption coefficient. This typically leads to about  $2 \times 10^6$  LTE background lines. The line profiles of these lines are taken to be depth-dependent profiles (with Voigt profiles for the strong lines and Gauss profiles for weak lines). We have verified in test calculations that the details of the LTE background line profiles and the threshold  $\Gamma$  do not have a significant effect on the model structure and the synthetic spectra. However, the LTE background lines should be included in detailed model calculations because their cumulative effect can change the structure and the synthetic spectra. In addition, we include about 2000 photo-ionization cross sections for atoms and ions (Verner & Yakovlev 1995).

PHOENIX is a full multi-level NLTE code, i.e., NLTE effects are considered self-consistently in the model calculations, including the radiative transfer calculations and the temperature corrections. Hauschildt & Baron (1995) have extended the numerical method developed by Hauschildt (1993) for NLTE calculations with a very detailed model atom of Fe II. In the calculations presented in this paper, we use a significantly enlarged set of NLTE species, namely H, He I–II, Mg II, Ca II, Ne I, C I–IV, N I–VI, O I–VI, S II–III, and Si II–III, (Hauschildt et al. 1997, for a complete list of NLTE species available in PHOENIX 9.1 see). Here, we do *not* use the NLTE treatment for Li I, Na I, Fe I–III, Co I–III and Ti I–III because these ionization stages are not important in metal-poor OB star atmospheres and particularly Fe, Co, and Ti NLTE would considerably increase the CPU time for the model calculations with little additional improvements in the results. We include a total of 2120 NLTE levels and 14,080 NLTE primary lines in the calculations presented here, nearly a factor of 5 more levels and lines than in our previous calculations (Hauschildt et al. 1996). The construction of the model atoms is described in (Hauschildt et al. 1997) and references therein.

## 2.1 NLTE Calculation Method

The large number of transitions that have to be included in realistic models of the NLTE line formation require an efficient method for the numerical solution of the multi-level NLTE radiative transfer and model calculation problem. The model atoms used here include more than 14,080 individual NLTE lines plus a large number of weak background transitions. Classical techniques, such as the complete linearization or the Equivalent Two Level Atom methods, are computationally prohibitive. PHOENIX performs its calculations in the co-moving frame for expanding atmospheres (e.g., stellar winds, novae and supernovae), therefore, approaches such as Anderson’s multi-group scheme (Anderson 1987; Anderson 1989) or extensions of the opacity distribution function method (Hubeny & Lanz 1995) cannot be applied. Simple approximations such as the Sobolev method, are very inaccurate in problems in which lines overlap strongly and make a significant continuum contribution (important for weak lines), as is the case for nova (and SN) atmospheres cf. (Hauschildt et al. 1996; Baron et al. 1996).

We use the multi-level rate-operator splitting (or pre-conditioning) method described by (Hauschildt 1993). This method solves the non-grey, spherically symmetric, special relativistic equation of radiative transfer in the co-moving (Lagrangian) frame using the operator splitting method de-

scribed in (Hauschildt 1992). Details of the method are described in (Hauschildt & Baron 1995), so we do not repeat the detailed description here. For all primary NLTE lines the radiative rates and the approximate rate operators (Hauschildt 1993) are computed and included in the iteration process. Secondary NLTE lines are included as background transitions for completeness but are insignificant for the model structure and the synthetic spectra (the model atoms have been explicitly constructed so that all important lines are primary lines).

## 2.2 Atmosphere Models

We have computed a small grid of spherically symmetric *static* models to investigate the effects of NLTE on the structure and the spectra of metal poor OB-stars. The models include the NLTE treatment as discussed above as well as the standard PHOENIX NLTE generalized equation of state and additional LTE background lines (about 2 million atomic lines). Aufdenberg et. al. (1998) showed that the *combined* effects of line blanketing and spherical geometry can dramatically change the short wavelength spectrum of the models, therefore, we calculated all models presented here using spherical geometry (incl. spherically symmetric radiative transfer). Models that include the effects of a stellar wind on the structure of the atmosphere and the emitted spectrum are currently being calculated (Aufdenberg et al, in preparation). The NLTE effects are included in both the temperature iterations (so that the structure of the models includes NLTE effects) and all radiative transfer calculations. For each primary NLTE line we add 3 to 5 wavelength points to the overall wavelength grid. This procedure typically leads to about 55,000–150,000 wavelength points for the model computations and the synthetic spectrum calculations. Test calculations have shown that the resulting overall wavelength grid is completely adequate for NLTE calculations in static and expanding media (Hauschildt & Baron 1995). We have also calculated LTE continuum and line blanketed models for comparison. In figure 1 we show a synthetic spectrum at the nominal resolution, illustrating the effect of low resolution on the appearance of the spectrum.

We compare our LTE and NLTE models to the Kurucz 92 LTE set of synthetic spectra in Figs. 2 and 3. The PHOENIX spectra have been convolved with a Gaussian kernel of 6Å half-width to make the resolutions of the different sets of spectra comparable. In general the spectra are very similar. We use an updated version of the Kurucz atomic line lists; this could explain the differences between the LTE models. In addition, the PHOENIX models allow for line scattering and NLTE (Fig. 3) whereas the Kurucz models are calculated using complete LTE (no line scattering).

## 3 RESULTS

All model atmospheres presented in this paper have  $\log(g) = 4.0$ . Three effective temperatures (A, B, and C respectively)  $T_{eff} = 38,000, 45,000, \text{ and } 55,000$  K, have been considered. For each of these  $T_{eff}$  we have computed models with 10%, 5% and 2% solar metal abundances(1-3, 4-6, 7-9 respectively). In each case NLTE and LTE line blanketed mod-

els as well as LTE continuum models were calculated. The models and the resulting ionization parameters  $q_0$ : the base ten-logarithm of the emission rate of HI Lyman continuum photons

$$q_0 = \log_{10} \left( 4\pi^2 \int_0^{\lambda_{L\alpha}} d\lambda \frac{F_{\lambda}\lambda}{hc} \right), \quad (1)$$

and  $q_1$  (helium continuum) are presented in table 1. In addition we have computed for each temperature a line blanketed LTE solar metallicity model (AS, BS, CS), to assess quantitative differences which could result from a contaminating population of young evolved stars that may be present in the HII region.

We start by considering low metallicity models. As expected, the resulting ionization photon fluxes are most sensitive to the temperature. The dependence in  $q_1$  on the metallicity is typically weak. The strongest variation is among the different model type themselves (LTE vs. NLTE). For the higher temperatures the differences in  $q_0$  and  $q_1$  are typically of order 0.02 or less. For models A1-9, the differences in  $q_1$  between LTE and NLTE models can be as large as 0.19, meaning that the amount of He ionizing flux differs by a factor of  $10^{0.19}$ . As the differences in  $q_0$  is only about 0.02, the implied difference is the ratio of helium-ionizing flux to hydrogen-ionizing flux is about  $10^{0.17} \sim 1.45$ .

We compare the spectra of the NLTE, LTE line blanketed and LTE continuum models for three effective temperatures in Figs. 4 to 6. The effects of line blanketing on the overall shape of the spectra is significant, even at the lowest metallicity that we have considered. The differences between LTE and NLTE spectra are smaller than the effects of line blanketing by itself. Longward of 1000 Å, NLTE effects on the spectra are small, especially near the threshold temperature of  $T_{\text{eff}} = 38,000$  and would thus have small if any impact on near-UV observations.

In figures 7 to 9 we show comparisons between solar metallicity spectra and spectra computed for 1/10 of the solar metallicity. In the solar metallicity spectra the metal lines are always stronger than in the spectra for 1/10 solar metallicity (though the Lyman edge is typically not quite as strong as in the 1/10 solar metallicity spectra). The differences in the value of  $q_1$  are 11%. This implies that if 10% of the stars are younger higher metallicity stars, the differences in the total ionizing number of photons exciting the surrounding nebula would be about 1%. However, the differences between the spectra are considerably more pronounced. The resulting effects from this fact have been studied recently by (Garacía-Vargas et. al. 1997), who found that the Wolf-Rayet contribution typically dominates this effect.

#### 4 CONCLUSIONS

Our synthetic spectra show that the predicted degree of helium ionization in GEHR could vary significantly depending on different model assumptions about the stellar atmospheres. In the end, the computed value of  $[\text{He}]/[\text{H}]$  in the nebula depends on the fraction of ionization contributed by the “relatively cool” hot stars, as well as the geometry of the HII region. As the number of recombinations in an HII region equals the number of ionization, one might expect

that the depths of the ionization zones for He and H would scale roughly as the cube root of the ionizing fluxes (only roughly because He-ionizing radiation can also ionize H). On the other hand, the uncertainties discussed in this paper, i.e. those due to the assumption of a *static* atmosphere, might be augmented by additional uncertainties in line blanketing effects, such as the existence of winds (Gabler et al., 1989, 1991, 1992; Najarro et al. 1996), shocks, etc., which are beyond the scope of this paper. The existence of additional uncertainties in the nebular dynamics, such as those implied by the presence of filaments, also need to be investigated farther. The extent to which the theoretical uncertainty can be gauged by scatter in the data is also hard to assess here, because much of it may be systematic.

*Acknowledgments:* Part of this work was carried while S.P. was a visiting Minerva fellow at the Max-Planck Institute für Astrophysik. The work was supported in part by US-Israel BSF grant 1802504, by NASA ATP grant NAG 5-3018 and LTSA grant NAG 5-3619 and by NSF grant AST-9720704 to UGA, and by NSF grant AST-9417242, NASA grant NAG5-3505 and an IBM SUR grant to the University of Oklahoma. Some of the calculations presented in this paper were performed on the IBM SP2 of the UGA UCNS, at the San Diego Supercomputer Center (SDSC) and the Cornell Theory Center (CTC), with support from the National Science Foundation. We thank all these institutions for a generous allocation of computer time.

#### REFERENCES

- Anderson, L. S. 1987, In *Numerical Radiative Transfer*, W. Kalkofen, editor, page 163, Cambridge University Press.  
 Anderson, L. S. 1989, *ApJ*, 339, 559.  
 Aufdenberg, J.P., Hauschildt, P. H. Shore, S.N. & Baron, 1998, *ApJ*, 498, 837.  
 Auer, L. & Mihalas, D., *ApJS*, 24, 193.  
 Baron, E., Hauschildt, P. H., Nugent, P., & Branch, D. 1996, *MNRAS*, 283, 297.  
 Baron, E. & Hauschildt, P. H. 1998, *ApJ*, 495, 370.  
 Dinerstein, H. L., & Shields, J. C. 1986, *ApJ*, 311, 45.  
 Dinerstein, H. L., & Shields, J. C. 1989, *The interstellar medium in galaxies*, 257.  
 Ferland G.J., 1996, Department of Physics and Astronomy Internal Report (University of Kentucky)  
 Gabler, R, Kudritzki, R. P. Puls, J. & PAuldrach, A. *A&A*, 226, 162.  
 Gabler, R, Kudritzki, R. P. & Mendez, R.H. *A&A*, 245, 587.  
 Gabler, R, Gabler A, Kudritzki, R. P. & Mendez, R.H. *A&A*, 265, 656.  
 Garacía-Vargas, M.L. & Díaz, A.I., 1994, *ApJS*, 91,553.  
 Garacía-Vargas, M.L. 1996, ASP conf. Proc. 98, 244.  
 Garacía-Vargas, M.L., González-Delgado, R.M., Pérez, E., Alloin, D., Díaz, A., & Terlevich, E., 1997, *ApJ*, 478, 112.  
 Hauschildt, P., Baron, E., Starrfield, S., & Allard, F. 1996, *ApJ*, 462, 386.  
 Hauschildt, P. H. 1992, *JQSRT*, 47, 433.  
 Hauschildt, P. H. 1993, *JQSRT*, 50, 301.  
 Hauschildt, P. H., & Baron, E. 1995, *JQSRT*, 54, 987.  
 Hauschildt, P. H., Schwarz, G. J., Baron, E., Starrfield, S., Shore, S., & Allard, F. 1997, *ApJ*, 490, 803.  
 Hauschildt, P. H., Baron, E., & Allard, F. 1997, *ApJ*, 483, 390.  
 Hauschildt, P. H., & Baron, E. 1998, *J. Computational and Applied Mathematics*, in press.  
 Hubeny, I., & Lanz, T. 1995, *ApJ*, 439, 875.  
 Husfeld, et al. 1984, *A&A* 134, 139.

- Kudritzki, R. P., A&A, 28, 103.  
Kudritzki, R. P., A&A, 52, 11.  
Kudritzki, R. P., Proc. 22nd Liege Conf. p.95  
Kudritzki, R. P., Saas Fe Lectures  
Kurucz, R., 1992, IAU Symp., 149, 225  
Kurucz, R., 1992, Kurucz CD-ROM No. 1  
Najarro et al. A&A 306, 892.  
Pagel, B., Simonson, E., Terlevich, R. J., & Edmunds, M. 1992, MNRAS, 255, 325.  
Sasselov, D., & Goldwirth, D. 1995, ApJL, 444, L5.  
Shields, J. C. 1990, ARA&A, 28, 525.  
Skillman, E. D. 1989, ApJ, 347, 883.  
Skillman, E. D., Terlevich, R. J., Garnett, D. R., & Terlevich, E. 1994, ApJ, 431, 172.  
Terlevich, E., Skillman E, D., & Terlevich, R. J. 1996, In *The Interplay between massive star formation, the ISM and Galaxy evolution*, Kunth et al., editor, page 395, (Frontiers:Singapore).  
Van der Hulst, E. 1988, A&A, 195, 38.  
Verner, D. A., & Yakovlev, D. G. 1995, A&AS, 109, 125.

**Table 1.** Models Input Parameters and Results. Cont stands for continuum LTE models, LTE for line blanketed LTE model and NLTE for NLTE line blanketed models

Model	Type	$T_{eff}$	$[M/H]$	$q_0$	$q_1$
A1	NLTE	38,000K	-1.	24.0443	23.1560
A2	LTE	38,000K	-1.	24.0232	22.9831
A3	Cont	38,000K	-1.	24.0226	23.0756
A4	NLTE	38,000K	-1.3	24.0351	23.1610
A5	LTE	38,000K	-1.3	24.0204	22.9928
A6	Cont	38,000K	-1.3	24.0307	23.0976
A7	NLTE	38,000K	-1.7	24.0311	23.1885
A8	LTE	38,000K	-1.7	24.0164	22.9959
A9	Cont	38,000K	-1.7	24.0292	23.0991
AS	LTE	38,000K	0	24.0640	22.9930
B1	NLTE	45,000K	-1.	24.5376	23.8949
B2	LTE	45,000K	-1.	24.5345	23.9063
B3	Cont	45,000K	-1.	24.5113	24.0245
B4	NLTE	45,000K	-1.3	24.5322	23.9171
B5	LTE	45,000K	-1.3	24.5345	23.9063
B6	Cont	45,000K	-1.3	24.5100	24.0246
B7	NLTE	45,000K	-1.7	24.5282	23.9497
B8	LTE	45,000K	-1.7	24.5247	23.9512
B9	Cont	45,000K	-1.7	24.5092	24.0246
BS	LTE	45,000K	0	24.5620	23.818
C1	NLTE	55,000K	-1.	24.9812	24.5081
C2	LTE	55,000K	-1.	24.9842	24.5065
C3	Cont	55,000K	-1.	24.9525	24.5860
C4	NLTE	55,000K	-1.3	24.9766	24.5197
C5	LTE	55,000K	-1.3	24.9789	24.5196
C6	Cont	55,000K	-1.3	24.9521	24.5858
C7	NLTE	55,000K	-1.7	24.9730	24.5389
C8	LTE	55,000K	-1.7	24.9734	24.5342
C9	Cont	55,000K	-1.7	24.9521	24.5859
CS	LTE	55,000K	0	25.0030	24.4670

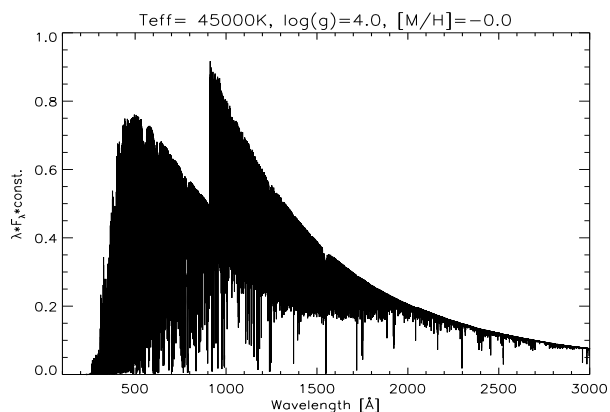


**Figure 1.** The NLTE spectrum for  $T_{\text{eff}} = 45,000$  K,  $\log(g) = 4.0$  and solar metallicity at the nominal resolution used in the model calculations.

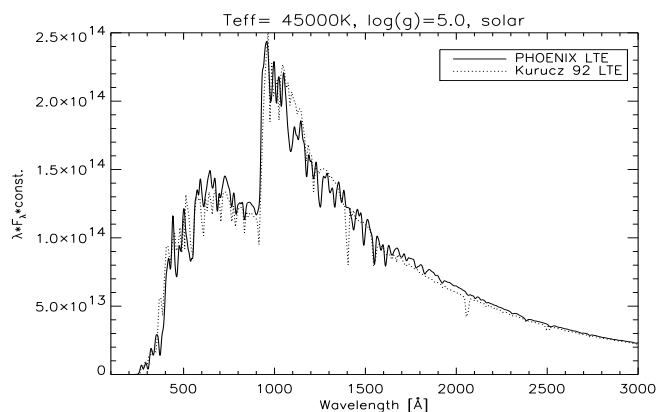


**Figure 3.** Comparison between a PHOENIX NLTE spectrum and a Kurucz 1992 LTE spectrum for  $T_{\text{eff}} = 45,000$  K,  $\log(g) = 5.0$  and solar metallicity. The PHOENIX spectrum has been degraded in resolution by convolving it with a Gaussian kernel with  $6\text{\AA}$  half-width.

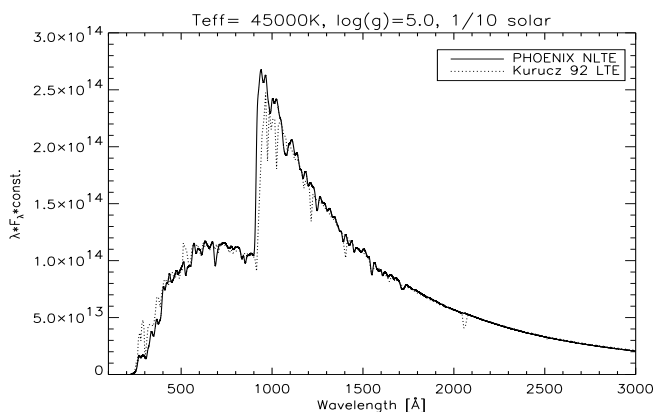


**Figure 2.** Comparison between a PHOENIX NLTE spectrum and a Kurucz 1992 LTE spectrum for  $T_{\text{eff}} = 45,000$  K,  $\log(g) = 5.0$  and  $1/10$  solar metallicity. The PHOENIX spectrum has been degraded in resolution by convolving it with a Gaussian kernel with  $6\text{\AA}$  half-width.

## 5 FIGURES

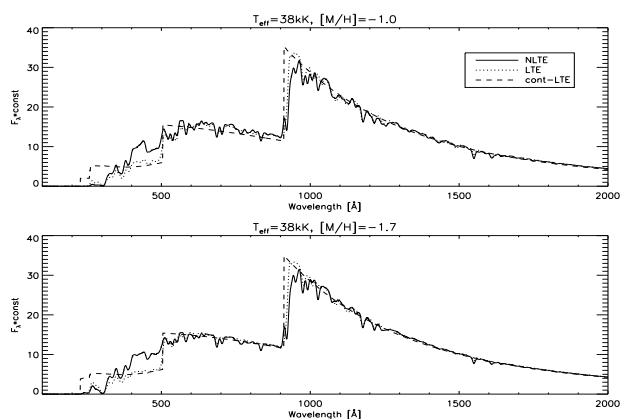


**Figure 4.** Models with  $T_{\text{eff}} = 38\text{kK}$ , Continuum LTE, Line LTE and NLTE models are overlaid. Top panel 10% solar metal abundance, bottom panel 2% solar metal abundance.

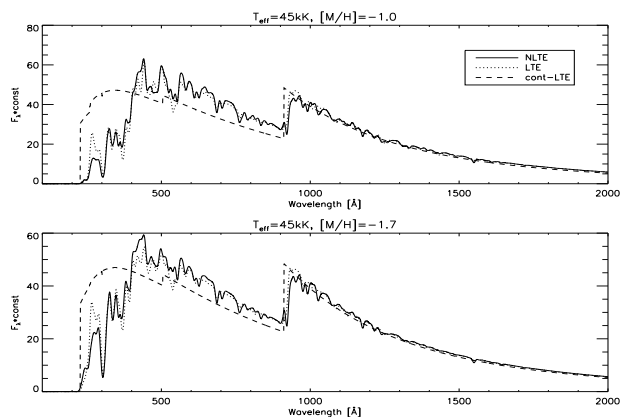


**Figure 5.** Models with  $T_{\text{eff}} = 45\text{kK}$ , Continuum LTE, Line LTE and NLTE models are overlaid. Top panel 10% solar metal abundance, bottom panel 2% solar metal abundance.

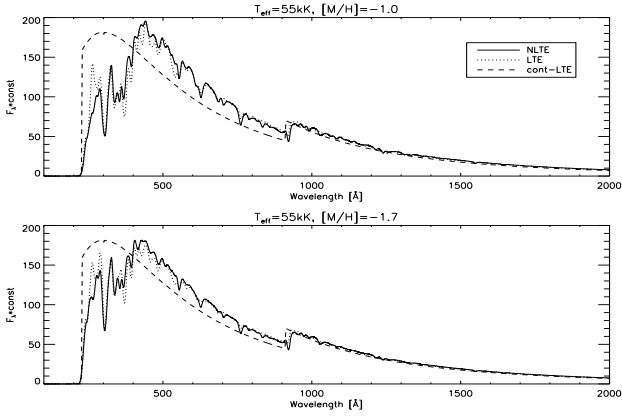


**Figure 6.** Models with  $T_{eff} = 55\text{kK}$ , Continuum LTE, Line LTE and NLTE models are overlaid. Top panel 10% solar metal abundance, bottom panel 2% solar metal abundance.

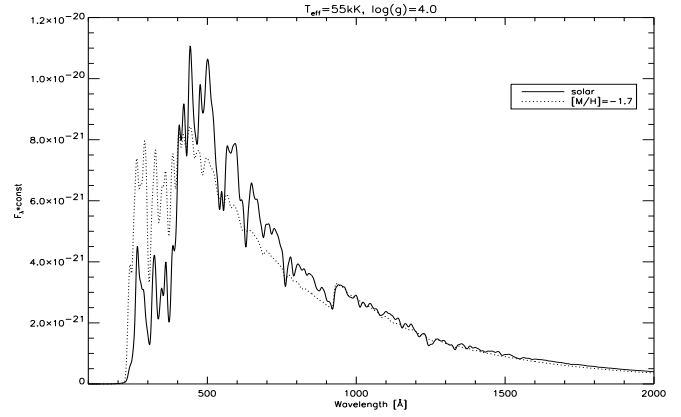


**Figure 9.** Comparison between Synthetic spectra for  $T_{eff} = 55\text{kK}$  for solar and 2% solar metal abundances.

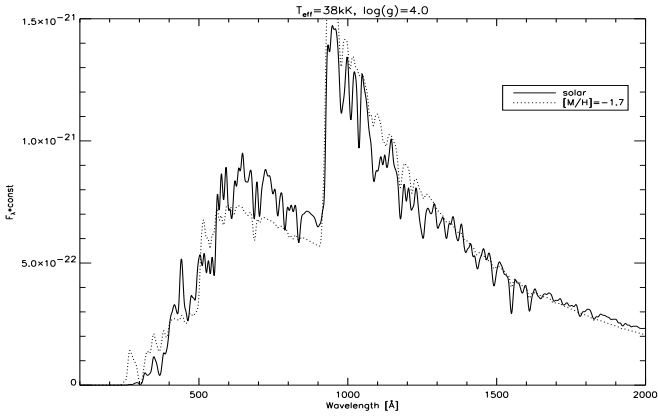


**Figure 7.** Comparison between Synthetic spectra for  $T_{eff} = 38\text{kK}$  for solar and 2% solar metal abundances.

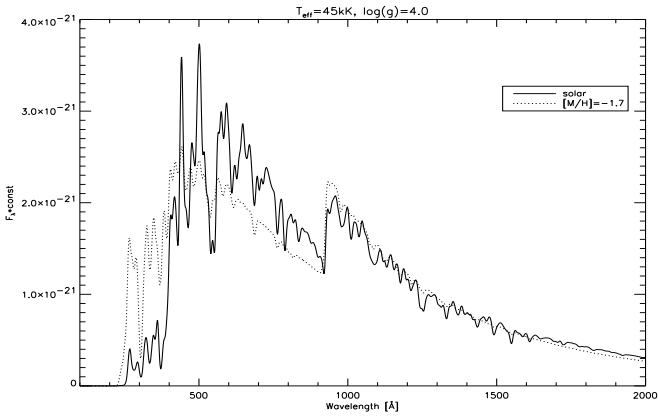


**Figure 8.** Comparison between Synthetic spectra for  $T_{eff} = 45\text{kK}$  for solar and 2% solar metal abundances.